ELSEVIER

Contents lists available at ScienceDirect

Journal of Electroanalytical Chemistry

journal homepage: www.elsevier.com/locate/jelechem



Detection of zwitterion at an electrified liquid-liquid interface: A chemical equilibrium perspective



Ran Chen, Andrew Brian McAllister, Mei Shen*

Department of Chemistry, University of Illinois at Urbana-Champaign, 600 South Mathews Avenue, Urbana, IL 61801, United States of America

ARTICLE INFO

Article history:
Received 22 March 2018
Received in revised form 4 May 2020
Accepted 23 May 2020
Available online 2 June 2020

Keywords:
Nanopipet
ITIES
Chemical equilibrium
Partition coefficient
Binding constant
Zwitterion
GABA
Octanoic acid
Octanoate
DB18C6

ABSTRACT

Ion transfer across the Interface between Two Immiscible Electrolyte Solutions (ITIES) has been successfully used for chemical sensing and the determination of the equilibrium constants of ion complexation reactions. Recently, we reported the detection of a zwitterion, gamma-aminobutyric acid (GABA), at nanoITIES where an organic acid was added into the oil phase as a pH modulator to enable the detection of the zwitterion [1]. Accompanying our first introduction of an organic acid to the oil phase of ITIES, apart from ion complexation equilibrium associated with the assisted ion transfer, additional equilibria are formed including acid-base and partition equilibria. Here, we studied the chemical equilibrium reactions involved in this system, where we measured the unknown equilibrium constants using conventional separation and electrochemical methods. We further demonstrated that how concentration of ion-ophore in the oil phase impacts the electrochemical reaction, which can be explained by Le Chatelier's principle.

1. Introduction

The Interface between Two Immiscible Electrolyte Solutions (ITIES) has become a powerful platform for chemical sensing, allowing the study of a variety of chemical reactions [2-10], such as interfacial catalysis [11,12], nanoparticle synthesis [13,14], neurotransmitter detection [15-22] and metal ion detection [23-27]. Accompanying electrochemical reaction at ITIES, various chemical equilibrium reactions occur, such as the partition between aqueous phase and oil phase, the ion complexation, etc. Understanding the fundamental aspects of the chemical equilibrium reactions involved in the ITIES studies is critical in developing better ITIES sensing platforms, and for carrying out chemical reactions at ITIES in a controlled manner. We recently introduced additional chemical equilibrium reactions in the design of ITIES electrodes, where we added an organic acid to the oil phase contained inside the pipet [1]. We successfully demonstrated the detection of a zwitterion, gammaaminobutyric acid (GABA), in biological aqueous pH by an interfacial protonation prior to the transfer of the resulting ion. However, several chemical equilibrium reactions are introduced accompanying the addition of the organic acid to the oil phase. These are shown in Fig. 1 and include dissociation of the organic acid inside oil and aqueous phases, respectively (reactions 1

We present here systematic study of the chemical equilibria involved in the ITIES measurements, where three fundamental types of chemical equilibrium reactions, i.e. acid-base, partition, and complexation, were intertwined within the electrochemical detection at ITIES. First, we used classical separation methods and cyclic voltammetry (CV) at ITIES to determine the unknown equilibrium constants. Secondly, we studied how the chemical equilibrium law (Le Chatelier's principle) modulates the electrochemical detection at ITIES.

2. Experimental section

2.1. Materials

 $\label{eq:magnesium} \begin{array}{lll} \text{Magnesium chloride hexahydrate (MgCl}_2 \cdot 6H_2O) \text{ was purchased} \\ \text{from } & \text{Amresco} & \text{(Solon, OH)}. & \text{Dibenzo-18-crown-6} & \text{(DB18C6)}, \end{array}$

and 3b), the partition of the organic acid between oil and aqueous phases (reaction 3a), the partition of proton between the oil and aqueous phases (reaction 4), the partition of the conjugate base of the organic acid between the oil and aqueous phases (reaction 5). Besides, proton complexation with the ion-ophore (reaction 2) and protonation of the zwitterion (reaction 6) also occur.

^{*} Corresponding author.

E-mail address: mshen233@illinois.edu. (M. Shen).

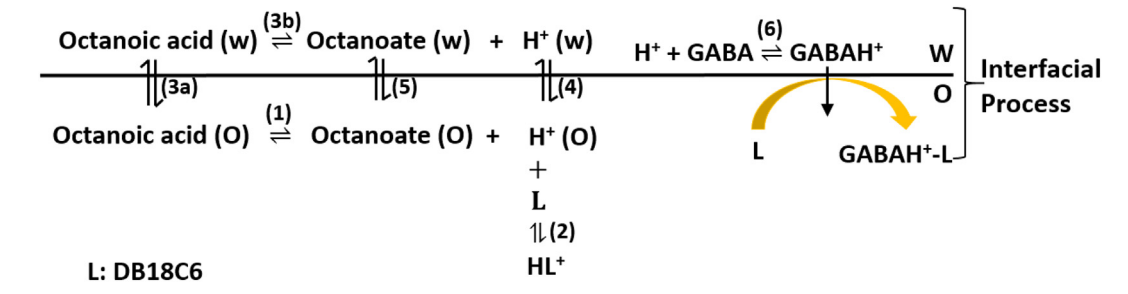


Fig. 1. The chemical equilibrium reactions involved in the detection of a zwitterion at nanoITIES electrode [1].

tetradodecylammonium (TDDA) chloride, tetrabutylammonium chloride (TBACl), 1, 2-dichloroethane (DCE), chlorotrimethylsilane, gamma-aminobutyric acid (GABA), sodium octanoate and sodium hydroxide, hydrochloride acid, and sulfuric acid were purchased from Sigma-Aldrich (St. Louis, MO). Potassium tetrakis(pentafluorophenyl) borate (TFAB) was obtained from Boulder Scientific Company (Mead, CO). The TFAB salt of TDDA (TDDATFAB) was prepared by metathesis [20]. Octanoic acid was purchased from the Aldrich Chemical Company, Inc. (Milwaukee, WI). Phenolphthalein was obtained from Fisher Scientific (Fair Lawn, NJ). Hydrochloric acid was obtained from Macron Fine Chemicals (Center Valley, PA). Deionized water obtained from Thermo Scientific (Middletown, VA). All reagents were used as received.

2.2. NanoITIES pipet electrode fabrication and characterization

Detailed nanoITIES pipet electrodes fabrication and characterization were reported recently [1,20–22,28–30]. Briefly, the nanopipets were fabricated through laser pulling of quartz capillaries (Sutter Instruments Novato, CA; 1 mm outer diameter, 0.7 mm inner diameter, 7.5 cm length) with a P-2000 Laser Puller (Sutter Instruments Novato, CA). The pulling parameters used in this experiment are shown below:

The nanopipet surface was treated by a chemical vapor silanization process using chlorotrimethylsilane. The nanopipets were backfilled with an electrolyte solution as detailed in the cell diagrams using a Hamilton syringe, and a gentle vibration was used to bring the filling solution to the orifice of the nanopiet.

2.3. Cyclic voltammetry measurements

All cyclic voltammetry (CV) measurements were performed either using a CHI760E potentiostat (CHI Instruments, Austin, TX) or a CHI902D potentiostat (CHI Instruments, Austin, TX). The oil phase inside the pipet was 1, 2-DCE. The background aqueous solution was 10 mM MgCl₂, which is commonly used in ITIES studies [1,16,17,20]. A Pt wire was inserted inside the nanopipet and an Ag/AgCl wire was placed in the aqueous phase as an outside reference electrode. A two-electrode configuration was used as reported previously [1,20–22,28–32], where a potential was applied between the inner Pt wire and the outer Ag/AgCl reference electrode. At applied positive potential, positive ions transfer from water to oil generating a positive current. TBA was added at the end of each experiment as an internal reference, and the potential with respect to the half-wave transfer potential of TBA, $E_{1/2, TBA}$, was reported. The half-wave transfer potential is the potential (x axis in CV) at half the diffusion limiting current (y axis in CV).

2.4. Determination of the partition coefficient of octanoic acid between water and DCE

The partition of octanoic acid between water and DCE was achieved by the shake flask method. We measured the amount of octanoic acid partitioned in the aqueous phase by titration. The detailed procedure is shown below. First, 15.00 mL of octanoic acid (which is equivalent to 9.465×10^{-2} mol) was added in a mixture of 40.0 mL aqueous solution (containing 10 mM MgCl₂) and 40.0 mL of DCE (containing 5 mM TDDATFAB). Then, the water / DCE mixture was vigorously shaken and separated in a separatory funnel. Lastly, the aqueous solution was collected and titrated with 0.00986 mol/L NaOH to measure the amount of octanoic acid distributed in aqueous phase. We used 0.5 wt% phenolphthalein solution as the indicator during the titration, which was prepared by dissolving 0.05 g of phenolphthalein in a mixture of 5 mL water and 5 mL ethanol. Before titration, we added 2 drops of the phenolphthalein solution. After that, we added the NaOH solution to the solution of octanoic acid slowly through the burette with sufficient stirring. The endpoint of the titration was marked by the color change of the solution from colorless to light pink, indicating the pH of the solution had become slightly basic. We further calculated the number of moles of octanoic acid partitioned in water, $n_{OA,W}$, using the following expression:

$$n_{OA,W} = c_{NaOH} \times V_{titration}$$

where c_{NaOH} is the concentration of NaOH solution, $V_{titration}$ is the volume of NaOH used in the titration. The number of moles of octanoic acid distributed in DCE, $n_{OA,O}$, can be further calculated as 9.465 \times 10⁻² mol - $n_{OA,W}$. Finally, we calculated the partition coefficient of octanoic acid between water and DCE using $P_{OA} = n_{OA,W} / n_{OA,O}$.

2.5. The determination of the partition coefficient of proton between water and DCF

The partition of proton between water and DCE was achieved by the shake flask method. The amount of proton partitioned in the aqueous phase was determined by pH measurements, and the partition coefficient of proton between water and DCE was further derived. The detailed procedure is shown below. First, 100 μL of concentrated HCl (12.1 mol/L) was added into 50.0 mL of 10 mM MgCl $_2$ solution. After mixing, the pH of this solution was measured by a pH meter (Accumet model-15, Fisher Scientific, Hapton, NH). We calculated the total number of moles of proton in the aqueous phase, $n_{proton,total}$ using this pH.

After measuring $n_{proton,\ total}$, we proceeded to the partition experiment to measure the amount of proton remained in the aqueous phase. Here, we mixed this aqueous solution of HCl with 50.0 mL DCE containing 5 mM TDDATFAB. After vigorous shaking and separation in a separatory funnel, the aqueous phase was collected and the pH was measured. We calculated the number of moles of proton partitioned in the aqueous phase, $n_{proton,\ W}$, from the pH. We further calculated the number of moles of proton in the organic phase, $n_{proton,\ O}$, using $n_{proton,\ O} = n_{proton,\ total} - n_{proton,\ W}$. Finally, we calculated the partition coefficient of proton between water and DCE, p_{proton} using $p_{proton} = n_{proton,\ W} / n_{proton,\ O}$.

2.6. The determination of partition coefficient of octanoate between water and $\frac{1}{2}$

The partition of octanoate between water and DCE was studied by the shake flask method. We calculated the amount of octanoate partitioned in

the aqueous phase from the amount of OH^- in the aqueous phase, which was determined from pH measurements. The procedure is detailed below. First, 0.1 M sodium octanoate in 10 mM MgCl₂ was prepared, and we added 50.0 mL of this solution (which contains 0.005 mol of sodium octanoate) to 50.0 mL DCE containing 5 mM TDDATFAB. This mixture was vigorously shaken and separated in a separatory funnel. Then we collected the aqueous phase and measured its pH. Afterwards, we used this pH value to calculate the OH^- concentrations in the aqueous phase, which was further used to calculate the number of moles of octanoate in water, $n_{octanoate, W}$, as detailed in the Results and Discussion section. The number of moles of octanoate in the organic phase, $n_{octanoate, O}$ is calculated to be 0.005 mol- $n_{octanoate, W}$. Finally, we calculated the partition coefficient of octanoate between water and DCE using $P_{octanoate} = n_{octanoate, W} / n_{octanoate, O}$.

2.7. Use of activity or concentration in the equilibrium constants determination

To calculate the equilibrium constants, we used the concentrations except pH related calculations considering pH $= -\log a$, where a is the activity of proton. We calculated the proton concentration from a as detailed in the results and discussion section.

2.8. Measurement of equilibrium constant for DB18C6 complexation with proton

Electrochemical measurements using ITIES electrodes have been successfully used to measure the equilibrium constants (β) of ionic complexation reactions, with methods pioneered by Girault and colleagues [33–36]. To determine the binding constant between an ionophore and an ion, we made several assumptions as reported in these studies: [37] 1) the ionophore is not water soluble (totally dissolved in the organic phase), and ion-ionophore complex does not form in water (the ion is confined in the aqueous phase), and the transfer occurs by the interfacial complexation mechanism; 2) The complexation / decomplexation reaction is much faster than the diffusion process; 3) The rates of transfer of all the species across the interface are much larger than the corresponding rates of diffusion; 4) The diffusion coefficient of all the species are the same in each phase; 5) The effects on the various concentrations due to incomplete electrolytic dissociation and ion pairing or adsorption at the interface are neglected. With the above assumptions, when ionophore (DB18C6) is in excess, the following equation applies for the complexation reaction between DB18C6 and proton: [33-36].

$$\Delta_O^W \phi_{DB18C6H+}^{1/2} = \Delta_O^W \phi_{H+}^{0\prime} - \frac{RT}{zF} ln \xi - \frac{RT}{zF} ln \beta + m \frac{RT}{zF} \ln c_{DB18C6,O}$$
 (7)

 $\Delta_O^W \phi_{DB18C6H^+}^{1/2}$ is the Galvani interfacial half-wave potential of the complex DB18C6H⁺, which can be measured through cyclic voltammetry. $\Delta_O^W \phi_{H^+}^{0'}$ is the formal Galvani potential of the non-assisted proton transfer,

which was reported to be 0.549 V [38]. $\xi = (\frac{D^O}{D^W})^{1/2}$ is approximated to be 1.12 for the water/DCE system [39], where D^O and D^W are the diffusion coefficients in the organic phase and water, respectively. $c_{DB18C6, O}$ is the concentration of DB18C6 in DCE, R is the gas constant, T is the temperature, z is the number of charges on the ion and here z=1 for proton, and F is

Faraday's constant. m is the stoichiometric ratio, and β is the equilibrium constant of the complexation between proton and DB18C6. According to Eq. (7), as the ionophore concentration $c_{DB18C6, O}$ varies, the measured $\Delta_{\rm D}$ $^{W}\phi_{\rm DB18C6H+}^{1/2}$ would also change linearly as a function of $\ln c_{DB18C6, O}$ and β can be obtained from the intercept of the linear regression.

2.9. Calculating the Galvani potential ($\Delta_O^W \phi_{DB18C6H+}^{1/2}$) from measured half-wave transfer potential ($E_{1/2,\ DB18C6H+} - E_{1/2,\ TBA}$)

In Eq. (7), we use Galvani potential $(\Delta_{O}^{W}\phi_{DB18CGH+}^{1/2})$ to calculate the binding constant, β . However, in the CV measurements, we reported the half-wave transfer potential with respect to the half-wave transfer potential of TBA, $E_{1/2,TBA}$. The conversion to Galvani potential can be achieved using the following equation: [35].

$$\Delta_{O}^{W} \phi_{DB18C6H+}^{1/2} - \Delta_{O}^{W} \phi_{TBA}^{0'} = E_{1/2,DB18C6H+} - E_{1/2,TBA}$$
 (8)

where $E_{1/2,\,DB18CGH^+}-E_{1/2,\,TBA}$ is the measured proton half-wave transfer potential with respect to $E_{1/2,\,TBA}$, and $\Delta_O^W \phi_{TBA}^{O'}$ is the formal Galvani potential for TBA. Plugging the reported $\Delta_O^W \phi_{TBA}^{O'}$ value of -0.225 V [40] into Eq. (8) transforms it into:

$$\Delta_O^W \phi_{DB18C6H+}^{1/2} = -0.225 \ V + \left(E_{1/2,DB18C6H+} - E_{1/2,TBA} \right) \tag{9}$$

3. Results and discussion

We first present here the determination of the unknown chemical equilibrium constants. Then we discuss in detail how the electrochemical detection on ITIES electrodes can be modulated by Le Chatelier's principle, i.e. the law of chemical equilibrium. We used the recently reported ITIES system as our model system, where an organic acid as a pH modulator was added into the organic phase contained inside the pipet to enable the detection of zwitterionic neurotransmitter (Cell 1) [1].

Cell 1: Pt | x mM DB18C6 + 5 mM TDDATFAB + 1, 2-DCE + 252 mM Octanoic acid || 10 mM MgCl₂ + y mM HCl | AgCl | Ag (x = 1 or 25; y = 0 or 1).

The chemical equilibrium reactions and known constants are listed in Table 1. As shown in Table 1, the equilibrium constants for reactions 3b (octanoic acid dissociation) and 6 (GABA protonation) can be calculated from the known pKa values [41,42]. For the rest of the 4 chemical equilibria, we measured the equilibrium constants in this work, as detailed later. To mimic the experimental condition of electrochemical measurements, we added 10 mM $\rm MgCl_2$ in the water phase, and 5 mM TDDATFAB in the DCE phase in the partition experiments [1]. We observed that the partition coefficients measured are different with and without the presence of electrolytes in the water and DCE phases.

3.1. Calculation of the partition coefficients of octanoic acid, proton, and octanoate between water and DCE

Partition coefficient of octanoic acid between water and DCE. The partition coefficient of octanoic acid between water and certain organic phase such as octanol has been reported [43]. However, no research has been done

Table 1 Chemical equilibrium reactions involved in zwitterion detection at ITIES (Cell 1, y = 0, x = 25) and the equilibrium constants for the electrochemical system.

Eq.	Equilibrium reaction	Equilibrium constant	Ref
(1)	$C_8H_{16}O_2$ (org) $\Rightarrow C_8H_{15}O_2^-$ (org) + H^+ (org) (octanoic acid dissociation in DCE)	1.29×10^{-5}	41
(2)	$L(org) + H^{+}(org) \rightleftharpoons LH^{+}(org)$ (DB18C6 complexation with proton)	166	Current work
(3a)	$C_8H_{16}O_2$ (org) $\Rightarrow C_8H_{16}O_2$ (aq) (octanoic acid partition between water and DCE)	3.32×10^{-3}	Current work
(3b)	$C_8H_{16}O_2\left(aq\right) \rightleftharpoons C_8H_{15}O_2^-\left(aq\right) + H^+\left(aq\right)$ (octanoic acid dissociation in water)	1.29×10^{-5}	41
(4)	H^+ (org) $\rightleftharpoons H^+$ (aq) (proton partition between water and DCE)	21.22	Current work
(5)	$C_8H_{15}O_2^-$ (org) $\Rightarrow C_8H_{15}O_2^-$ (aq) (octanoate partition between water and DCE)	3.07×10^{-2}	Current work
(6)	$H^+ + GABA = GABAH^+$ (GABA binding with proton)	3.39×10^{4}	42

with DCE as the organic phase. Here, we present the first measurement of the partition coefficient of octanoic acid between water and DCE. The amount of octanoic acid partitioned in the aqueous phase, $n_{OA,\ W}$, was determined through acid-base titration to be 3.13 ($\pm\,0.03$) $\times\,10^{-4}$ mol; and the amount of octanoic acid remained in DCE after partition, $n_{OA,\ O}$, was further calculated to be 9.43 ($\pm\,0.00$) $\times\,10^{-2}$ mol, based on 9.465 $\times\,10^{-2}$ (total amount) – 3.13 ($\pm\,0.03$) $\times\,10^{-4}$ mol. We finally calculated the partition coefficient of octanoic acid between water and DCE ($n_{OA,\ W}$ / $n_{OA,\ O}$) to be 3.32 ($\pm\,0.03$) $\times\,10^{-3}$. This value is close to the reported partition coefficient of 8.91 $\times\,10^{-4}$ between water and octanol [43].

Partition coefficient of proton between water and DCE. To determine the partition coefficient of proton, 50 mL DCE was added to 100 μ L of concentrated HCl (12.1 mol/L) in 50 mL MgCl $_2$ aqueous solution, and then partition of proton between aqueous phase and DCE phase was carried out. We first measured the pH of the aqueous phase before and after partition, respectively, to calculate the $n_{proton\ total}$ (before partition) and $n_{proton\ W}$ (after partition). Then we calculated the amount of proton in the organic phase using $n_{proton\ total}-n_{proton\ W}$, and eventually calculated the partition coefficient, as detailed in Table 2. The measured pH in the aqueous phase was 1.74 (±0.00) and 1.76 (±0.00) before and after the partition, respectively. We calculated the activity of proton from pH values, followed by calculating the proton concentration via activity / activity coefficient.

The activity coefficient, γ , was estimated based on the extended Debye-Hückel model: [44].

$$\log \gamma_i = -A \frac{z_i^2 \sqrt{I}}{1 + B \times a_i \times \sqrt{I}} \tag{10}$$

where $A = 0.51 \text{ M}^{-1/2}$, $B = 3.3 \text{ M}^{-1/2} \text{ nm}^{-1}$, a_i is the radius of the ion in nanometer (= 0.9 nm for H⁺⁴⁴), z_i is the charge of the ion, and I is the total ionic strength in the solution in mol/L. I was calculated as:

$$I = \frac{1}{2} \sum_{i} z_i^2 C_i \tag{11}$$

with C_i being the concentration of the ion in mol/L and z_i being the charge of the ion as mentioned above. The ionic strength of the aqueous solution before adding HCl (originally contained 10 mM MgCl₂) is 0.03 M. I contribution from the added HCl was further estimated from the measured pH to be \sim 0.02 M (\sim 0.01 M from H $^+$ and \sim 0.01 M from Cl $^-$). Thus the total ionic strength was estimated to be \sim 0.05 M. Using Eq. 10, the activity coefficient γ_{H+} was calculated to be 0.85. Note that, γ_{H+} of 0.85 was calculated based on the estimated I of 0.05 M, and we further confirmed that this estimated I of 0.05 M is correct. Using calculated γ_{H+} , from the measured pH of 1.76 (\pm 0.00) using estimate I, the concentration of proton after partition was calculated to be 2.04 (\pm 0.02) \times 10 $^{-2}$ mol/L. This means I contribution from the added HCl was \sim 0.0204 mol/L (\sim 0.0102 mol/L from H $^+$ and \sim 0.0102 mol/L from Cl $^-$), resulting a total I of 0.0504 mol/L,

Table 2Determination of proton partition coefficient between water and DCE.

Parameter	Calculation process	Value
pH of aqueous phase before partition $n_{proton, \ total}$ / mol	measured experimentally 50.0 mL \times 10 ^{-1.74} \pm 0.005	1.74 (± 0.0) 1.07 (± 0.01) × 10^{-3}
pH of aqueous phase after partition $n_{proton, W}$ / mol	mol/L / 0.85 measured experimentally $50.0 \text{ mL} \times 10^{-1.76}$ ± 0.005	1.76 (±0.00) 1.02 (± 0.01) × 10^{-3}
$n_{proton, O}$ / mol partition coefficient of proton	mol/L / 0.85 $n_{proton, total} - n_{proton, W}$ $n_{proton, W} / n_{proton, O}$	4.82 (± 0.93) × 10 ⁻⁵ 21.2 (± 2.2)

Number of moles for proton in total, in aqueous, and in oil phase (DCE) was expressed as $n_{proton,\ total}$, $n_{proton,\ W}$, and $n_{proton,\ O}$, respectively.

consistent with the estimated I of \sim 0.05 M. In the case when the calculated I is found to be different from the estimated I, we would adjust the estimated I and calculate the corresponding γ_{H+} again as described above until the calculated I is consistent with its estimation.

Once the concentration of proton is calculated, the number of moles of proton ($n_{proton,\ W}$) after partition in the aqueous solution (50.0 mL) is calculated to be $1.02\ (\pm\ 0.01)\times 10^{-3}$ mol. Likewise, the total number of moles of proton before partition ($n_{proton,\ total}$) is calculated to be $1.07\ (\pm\ 0.01)\times 10^{-3}$ mol. Following that, the number of moles of proton partitioned in the organic phase ($n_{proton,\ O}$) is calculated using $n_{proton,\ total}$ - $n_{proton,\ W}$ to be $4.82\ (\pm\ 0.93)\times 10^{-5}$ mol. Finally, the partition coefficient for proton partitioning between water and DCE, $n_{proton,\ W}/n_{proton,\ O}$, is calculated to be $21.2\ (\pm\ 2.2)$.

Partition coefficient of octanoate between water and DCE. To determine the partition coefficient of octanoate between water and DCE, 0.005 mol of sodium octanoate was partitioned between the aqueous phase and DCE phase. We first measured the concentration of OH $^-$, c_{OH} , based on the pH of the aqueous solution after partition. Then the concentration of octanoate in aqueous phase, $c_{octanoate,\ W_i}$ after partitioning was calculated from c_{OH} based on its hydrolysis reaction:

$$C_8H_{15}O_2^- (aq) + H_2O (aq) \rightleftharpoons C_8H_{16}O_2 (aq) + OH^- (aq)$$
 (12)

The equilibrium constant of reaction (12), K_B , was obtained using $K_B = K_W / K_A$. K_A (1.29 \times 10⁻⁵) is the equilibrium constant of octanoic acid dissociation (3b) and K_W is the ionic product of water. K_B is calculated to be $10^{-14} / (1.29 \times 10^{-5}) = 7.76 \times 10^{-10}$. The activity coefficient γ_{OH} was calculated to be 0.835 using similar methods as the determination of γ_{H+} . The activity of hydroxide, a_{OH} , is $10^{8.10-14}$, calculated from the measured pH of 8.10 (after partition). c_{OH} was further calculated by $a_{OH} / \gamma_{OH} = 10^{8.10-14} / 0.835 \, \text{mol/L} = 1.52 \times 10^{-6} \, \text{mol/L}$. Then $c_{octanoate}$, γ_{OH} was calculated from γ_{OH} as detailed below.

$$\begin{split} K_B = 7.76 \times 10^{10} & \quad C_0 H_{18} O_2^- \left(aq \right) + H_2 O \left(aq \right) \rightleftharpoons C_0 H_{16} O_2 \left(aq \right) + OH^- \left(aq \right) \\ \text{Initial concentration (moVL):} & \quad c_{\text{extroware, } W} & 1 & 0 & \approx 0 \\ \text{Change (moVL):} & \quad - c_{OH} & \quad - c_{OH} & < c_{OH} & \approx c_{OH} \\ \text{Final concentration (moVL):} & \quad c_{\text{extroware, } W} - c_{OH} & 1 - c_{OH} & c_{OH} & \approx c_{OH}. \end{split}$$

 $K_B = c_{OH-} \times c_{OH-} / (c_{octanoate, W} \times 1)$, and was calculated to be 7.76 imes 10^{-10} in above section. pH of aqueous solution after partition was measured to be 8.10 (\pm 0.03). Plugging c_{OH} of 1.52 \times 10⁻⁶ (calculated above) into K_B expression, $c_{octanoale,\ W}$ is calculated to be 2.97₃ \times 10⁻³. Total concentration of octanoate partitioned in the aqueous phase is the combined concentration of octanoate and octanoic acid, which approximates $c_{octanoate}$. $_W + c_{OH-} = 2.97_3 \times 10^{-3} + 1.52 \times 10^{-6} \approx 2.97_5 \times 10^{-3} \,\text{mol/L}$ (based on the above equation). Following this, we calculated the number of moles of octanoate partitioned in 50 mL of aqueous solution: $n_{octaoate, W} = 50.0$ mL \times 2.97₅ \times 10⁻³ mol/L = 1.49 \times 10⁻⁴ mol. The total moles of added octanoate before partition ($n_{octanoate,total}$) was 50.0 mL \times 0.10 mol/L = 5.0×10^{-3} mol. Then octanoate partitioned in the organic phase, $n_{octanoate,O}$, was calculated to be 5.0 \times 10⁻³ mol ($n_{octanoate,total}$) - 1.49 \times 10⁻⁴ mol ($n_{octanoate, W}$) = 4.85 \times 10⁻³ mol. Finally, the partition coefficient of octanoate, $n_{octanoate,W}$ / $n_{octanoate,O}$, is calculated to be 3.07 (\pm $0.05) \times 10^{-2}$. This value is much smaller than that of proton measured above, likely due to the hydrophobicity of the long carbon chain in the octanoate ion.

3.2. Equilibrium constant of DB18C6 complexation with proton, β

To the best of our knowledge, the equilibrium constant of DB18C6 complexation with proton in DCE phase, β , has not been reported. Here, we measured β based on CVs of DB18C6 assisted proton transfer at ITIES electrodes (methods detailed in experimental section). Briefly, we measured DB18C6-assisted proton transfer CVs with different concentrations of DB18C6 in the oil phase, $c_{DB18C6, O}$, and analyzed the linear regression of Δ_D $\frac{W_0^{1/2}}{DB18C6H} + vs \ln c_{DB18C6, O}$ to determine β .

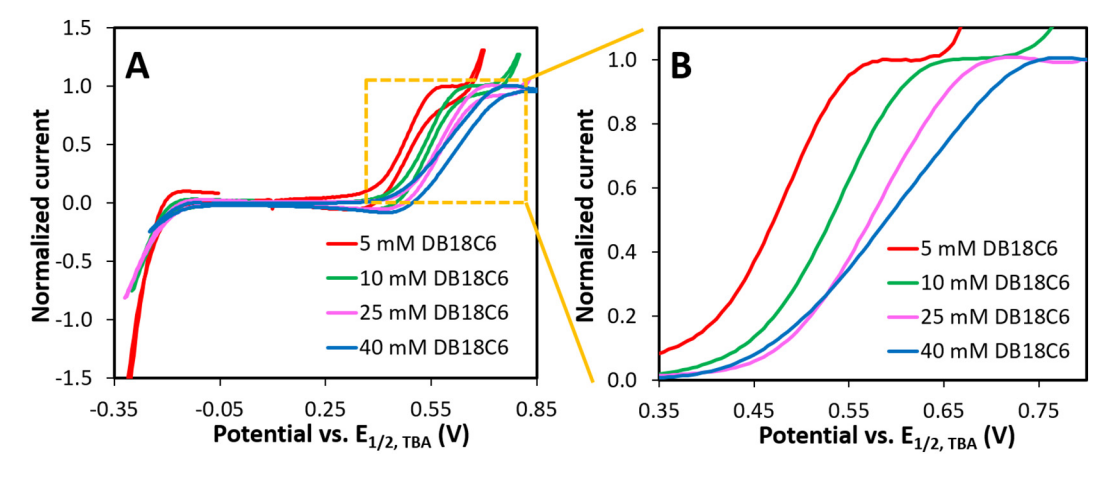


Fig. 2. CVs of the assisted proton transfer with different concentrations of DB18C6 (A) and its zoom in view (B), where only the forward waves were shown for easy visualization. The cell diagram used for the determination of β was shown below:

Cell 2: Pt | x mM DB18C6 + 5 mM TDDATFAB +1, 2-DCE | 10 mM MgCl₂ + 1 mM HCl | AgCl | Ag (x = 5, 10, 25 and 40)

The CVs of DB18C6-assisted proton transfer were shown in Fig. 2. $c_{DB18C6,\ O}$ was varied to be 5, 10, 25 and 40 mM. All potential was reported with respect to the half-wave transfer potential of TBA, $E_{1/2,\ TBA}$. CVs of different $c_{DB18C6,\ O}$ are plotted in Fig. 2A and zoomed in Fig. 2B. As shown in Fig. 2B, when the $c_{DB18C6,\ O}$ increases, the half-wave potential of the assisted proton transfer becomes more positive. We plotted $\Delta_O^W \phi_{DB18C6H^+}^{1/2}$ as a function of $\ln c_{DB18C6,O}$ in Fig. 3, and a good linear correlation between $\Delta_O^W \phi_{DB18C6H^+}^{1/2}$ and $\ln c_{DB18C6,O}$ was observed. The linear regression equation is:

$$\Delta_O^W \phi_{DB18C6H+}^{1/2} = -0.413(\pm 0.020) + 0.0262(\pm 0.005) \ln c_{DB18C6,0}$$
 (13)

where the slope of 0.0262 matches well the theoretical value of 0.026 assuming a 1:1 stoichiometric ratio between DB18C6 and proton. From the intercept of -0.413 (\pm 0.020) V, we calculated $ln\beta$ to be 5.11 (\pm 0.60). This further gives a β value of 166, similar to the β value of 5370 reported for DB18C6 complexation with proton measured in acetonitrile [45].

3.3. Tuning electrochemical reaction at ITIES via Le Chatelier's principle

We present here how the chemical equilibrium can modulate the ion transfer reaction at the electrified ITIES via Le Chatelier's principle

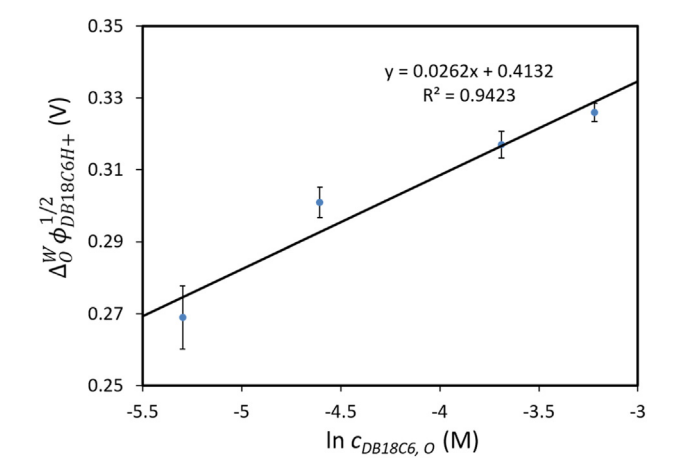


Fig. 3. Determining the equilibrium constant of DB18C6 complexation with proton. Plot of $\Delta_{O}^{N}\phi_{DB18C6H+}^{VS}$ with respect to $\ln c_{DB18C6, O}$.

(equilibrium law). We varied parameters involved in other equilibria including the DB18C6 concentration in oil phase, $c_{DB18C6,\ O}$, and proton concentration in aqueous solution, $c_{proton,\ W}$ to modulate the transfer of octanoate. The CV results are shown in Fig. 4, where Figs. 4A and 4C correspond to $c_{DB18C6,\ O}$ of 25 mM and Fig. 4B corresponds to $c_{DB18C6,\ O}$ of 1 mM. In each figure, the black solid curve and the red dashed curve represent the CVs before and after adding 1 mM proton, while the green dotted curve is the control with no octanoic acid present in the oil phase. The basic cell diagrams of Fig. 4 are shown below:

Pt | x mM DB18C6 + 5 mM TDDATFAB + z mM octanoic acid +1, 2-DCE | 10 mM MgCl₂ + 1 mM TBACl + y mM proton | AgCl | Ag

where x, y are $c_{DB18C6,O}$ and $c_{proton,W}$, and z is the concentration of octanoic acid in oil phase. The source of proton is HCl in Figs. 4A and 4B, and H₂SO₄ in Fig. 4C. The detailed variables for each plot are shown in Table 3 below:

We first did control experiments without octanoic acid in oil phase to confirm that the nanoITIES electrodes function well by observing the CV of an added standard compound, TBA. As shown in Fig. 4, well defined CVs (green dotted curves) corresponding to TBA transfer were observed, and the transfer of Cl $^-$ from water to oil phase occurred starting around $-0.2\,\rm V$. Then we added octanoic acid to the oil phase, the observed transfer of octanoate from water to oil phase leads to additional current on top of the Cl $^-$ transfer signal, as shown in the black solid and red dashed curves.

We further demonstrated how $c_{proton,\ W}$ modulates octanoate transfer from water to oil phase very differently, depending upon $c_{DB18C6,\ O}$. We found that when $c_{DB18C6,\ O}$ is 25 mM, increasing $c_{proton,\ W}$ does not cause a significant change in the octanoate transfer (red dashed curve essentially overlaps with black solid curve in Fig. 4A). In contrast, when $c_{DB18C6,\ O}$ is 1 mM (Fig. 4B), increasing $c_{proton,\ W}$ causes drastic shift of octanoate transfer in potential. Note that, the slight current increase in red dashed curve in Fig. 4A compared to black solid curve at potential ranging from $-0.15\ V$ to $-0.25\ V$ is likely due to the increased concentration of Cl $^-$ from the added HCl as source of proton. This was confirmed in Fig. 4C, where 0.5 mM H₂SO₄ was added instead of 1 mM HCl, and the red dashed curve overlapped perfectly with the black solid curve. The result in Fig. 4C again demonstrates that when $c_{DB18C6,\ O}$ is 25 mM, increasing $c_{proton,\ W}$ does not affect the transfer of octanoate.

Fig. 4 suggests that $c_{DB18C6,\ O}$ plays a significant role in octanoate transfer from water to oil phase at electrified ITIES. A possible explanation for this is shown in Scheme 1, where electrochemical detection of ions at ITIES was modulated via Le Chatelier's principle. Initial proton concentration in the oil phase, $c_{proton,\ O}$, is \sim 1.8 mM without considering all other chemical equilibria. Thus $c_{DB18C6,\ O}$ of 25 mM is in excess compared to $c_{proton,\ O}$ of 1.8 mM. This causes proton complexation reaction with DB18C6 (reaction 2) shift to the right, resulting in consumption of H⁺ (org). Decreased H⁺ (org) further suppressed H⁺ partition from oil to

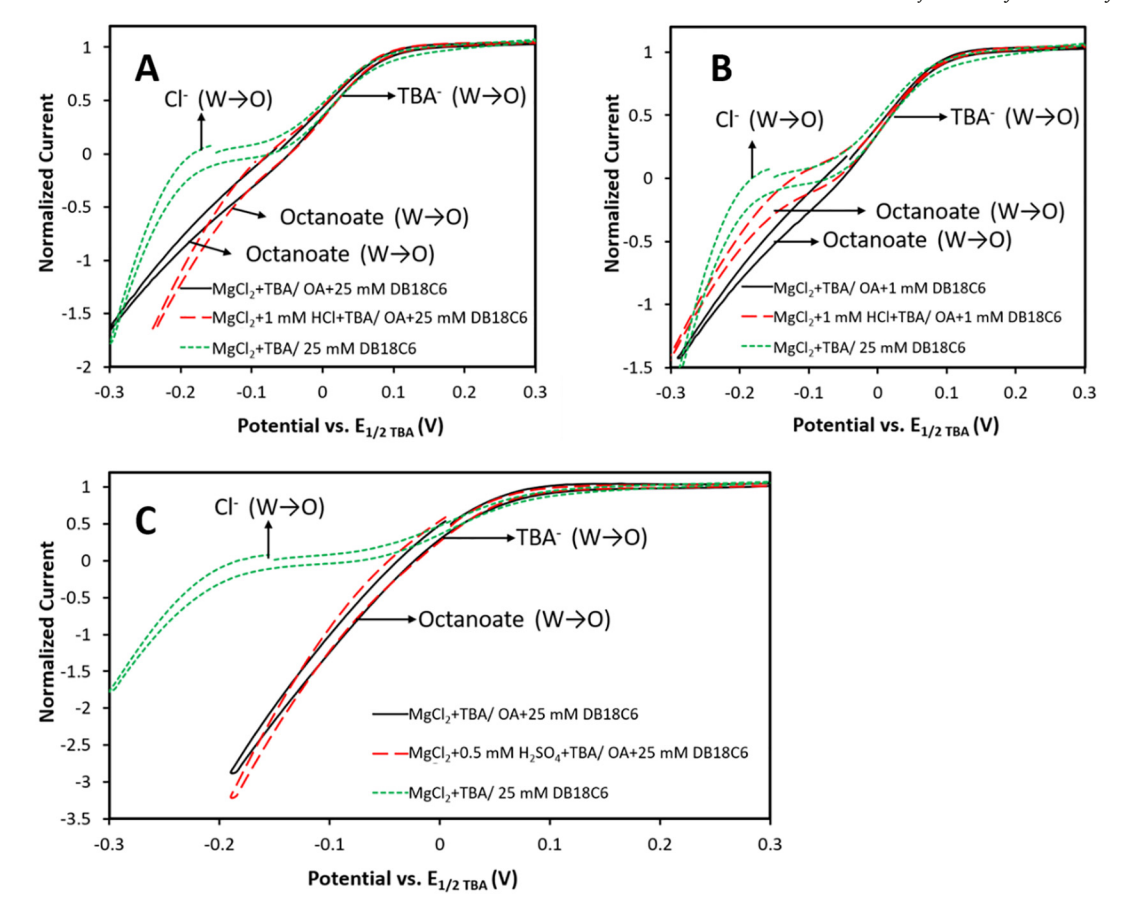


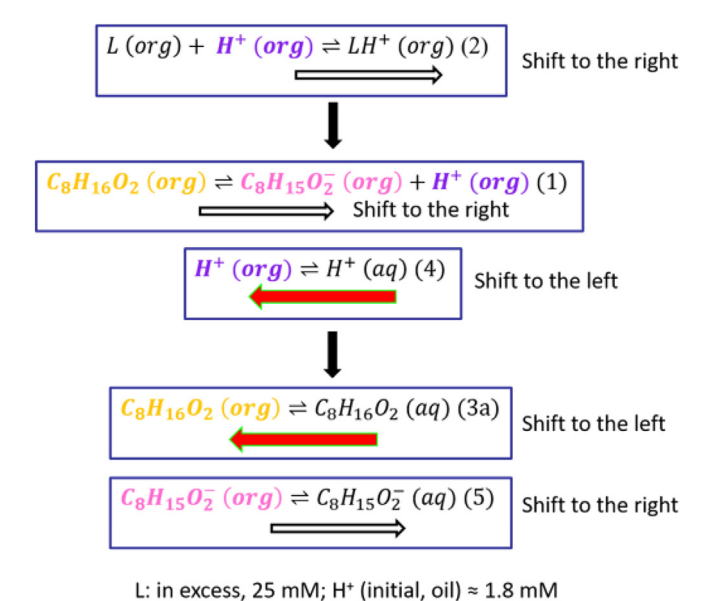
Fig. 4. (A) and (B): CVs with presence of octanoic acid before adding 1 mM HCl (black solid curve) and after adding 1 mM HCl (red dashed curve). (C): CVs with presence of octanoic acid before adding 0.5 mM H₂SO₄ (black solid curve) and after adding 0.5 mM H₂SO₄ (red dashed curve).

Table 3 Composition of the cell diagrams (x, y, z values) in Fig. 4.

Fig. 4A	Fig. 4B	Fig. 4C
x = 25	x = 25	x = 25
y = 0	y = 0	y = 0
z = 0	z = 0	z = 0
x = 25	x = 1	x = 25
y = 0	y = 0	y = 0
z = 252	z = 252	z = 252
x = 25	x = 1	x = 25
y = 1 (HCl)	y = 1 (HCl)	$y = 1 (H_2SO_4)$
z = 252	z = 252	z = 252
	x = 25 y = 0 z = 0 x = 25 y = 0 z = 252 z = 252 z = 25 z = 25	x = 25 x = 25 $y = 0 y = 0$ $z = 0 z = 0$ $x = 25 x = 1$ $y = 0 y = 0$ $z = 252 z = 252$ $x = 25 x = 1$ $y = 1 (HCl) y = 1 (HCl)$

water (reaction 4), as well as facilitates octanoic acid dissociation in DCE (reaction 1) consuming octanoic acid (org). Consequently, decreasing octanoic acid (org) further shifts octanoic acid partition from DCE to water (reaction 3a) to the left. As a result, the amount of octanoic acid partitioned into the aqueous phase is reduced. Thus, the octanoate in the aqueous solution mainly comes from its partition from DCE to water (reaction 5). This explains why when $c_{DB18CG,\ O}$ is 25 mM, increasing $c_{proton,\ W}$ does not modulate the transfer of octanoate (Figs. 4A and 4C).

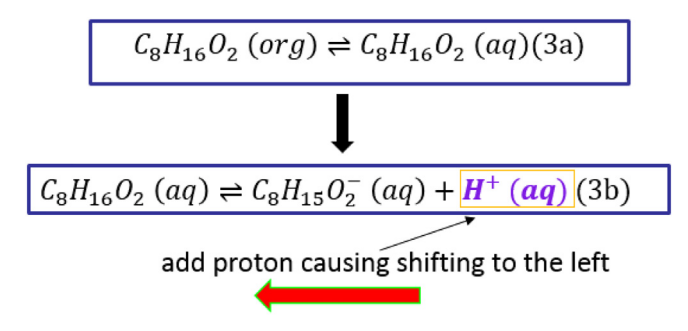
In contrast, when $c_{DB18C6,\ O}$ is 1 mM, the above-described equilibria shifts do not occur, resulting significant occurrence of octanoic acid partition from oil to water (reaction 3a). Partitioned octanoic acid to water further dissociates to generate octanoate and proton (reaction 3b). When we added $c_{proton,\ W}$, octanoic acid dissociation reaction (3b) gets shifted to the left, producing less octanoate in water (Scheme 2). As a result, we observed less octanoate transfer from water to DCE at electrified ITIES (Fig. 4B), namely octanoate transfer from water to oil was shifted in potential to the left side (red dashed curve compared to black solid curve).



Scheme 1. Mechanism of the modulation of octanoate transfer to explain why when $c_{DB18C6,\ O}$ is 25 mM, increasing $c_{proton,\ W}$ does not modulate the transfer of octanoate (Figs. 4A and 4C).

4. Conclusion

We have studied the chemical equilibrium reactions involved in the recently introduced ITIES electrode design. Several equilibrium constants



Scheme 2. Mechanism of the modulation of octanoate transfer to explain why when $c_{DB18G6, O}$ is 1 mM, increasing $c_{proton, W}$ modulates the transfer of octanoate (Fig. 4B).

have been measured for the first time. We measured the equilibrium constant of DB18C6 complexation with proton in DCE, with $h\beta$ being 5.11 (\pm 0.60), using cyclic voltammetry at nanoITIES electrode. The partition coefficients for octanoic acid, octanoate and proton partitioning between water and DCE were determined to be 3.32 (\pm 0.03) \times 10 $^{-3}$, 3.07 (\pm 0.05) \times 10 $^{-2}$ and 21.2 (\pm 2.2), respectively. We further showed the power of tuning chemical equilibria based on Le Chatelier's principle to modulate electrochemical reaction at ITIES. With added excess ionophore in the oil phase, the partition of organic acid from oil phase into aqueous phase was suppressed. The present study demonstrates the versatility of ITIES in electrochemical analysis. The experimental findings presented here can provide insights for future design of ITIES platform for its broad application in chemical sensing, synthesis, interfacial reactions and catalysis.

Declaration of Competing Interest

The authors declare no conflict of interest.

Acknowledgement

We appreciate the funding support for this research from the National Science Foundation with a CAREER award (CHE 19-45274) to M. Shen.

References

- [1] N.T. Iwai, M. Kramaric, D. Crabbe, Y. Wei, R. Chen, M. Shen, GABA Detection with nano-ITIES pipet electrode: a new mechanism, water/DCE-octanoic acid interface, Anal. Chem. 90 (2018) 3067–3072.
- [2] H.H. Girault, Electrochemistry at Liquid/Liquid Interfaces, in: A.J. Bard, G. Cynthia (Eds.), Electroanalytical Chemistry: A series of Advances: volume 23. CRC Press, Taylor&Francis Group, Boca Raton, FL, 2010.
- [3] P. Vanysek, L. Ramirez, Interface between two immiscible liquid electrolytes: A review, J. Chil. Chem. Soc. 53 (2008) 1455–1463.
- [4] Y. Shao, M.V. Mirkin, Voltammetry at micropipet electrodes, Anal. Chem. 70 (1998) 3155–3161.
- [5] S. Amemiya, J. Kim, A. Izadyar, B. Kabagambe, M. Shen, R. Ishimatsu, Electrochemical sensing and imaging based on ion transfer at liquid/liquid interfaces, Electrochim. Acta 110 (2013) 836–845.
- [6] G. Taylor, H.H. Girault, Ion transfer reactions across a liquid—liquid interface supported on a micropipette tip, J. Electroanal. Chem. 208 (1986) 179–183.
- [7] S. Liu, Q. Li, Y. Shao, Electrochemistry at micro- and nanoscopic liquid/liquid interfaces, Chem. Soc. Rev. 40 (2011) 2236–2253.
- [8] A. Berduque, A. Sherburn, M. Ghita, R.A.W. Dryfe, D.W.M. Arrigan, Electrochemically modulated liquid – liquid extraction of ions, Anal. Chem. 77 (2005) 7310–7318.
- [9] D.W.M. Arrigan, E. Alvarez de Eulate, Y. Liu, Electroanalytical opportunities derived from ion transfer at interfaces between immiscible electrolyte solutions, Aust. J. Chem. 69 (2016) 1016–1032.
- [10] P.J. Rodgers, S. Amemiya, Y. Wang, M.V. Mirkin, Nanopipet voltammetry of common ions across the liquid-liquid interface. Theory and limitations in kinetic analysis of nanoelectrode voltammograms, Anal. Chem. 82 (2010) 84–90.
- [11] Y. Shao, M. Mirkin, J. Rusling, Liquid/liquid interface as a model system for studying electrochemical catalysis in microemulsions. Reduction of trans-1,2dibromocyclohexane with vitamin B12, J. Phys. Chem. B 101 (1997) 3202–3208.
- [12] A.N.J. Rodgers, R.A.W. Dryfe, Oxygen reduction at the liquid-liquid interface: bipolar electrochemistry through adsorbed graphene layers, Chem. Electro. Chem. 3 (2016) 472–479.
- [13] G.C. Gschwend, E. Smirnov, P. Peljo, H.H. Girault, Electrovariable gold nanoparticle films at liquid-liquid interfaces: from redox electrocatalysis to Marangoni-shutters, Faraday Disc. 199 (2017) 565–583.

- [14] A.N.J. Rodgers, S.G. Booth, R.A.W. Dryfe, Particle deposition and catalysis at the interface between two immiscible electrolyte solutions (ITIES): a mini-review, Electrochem. Commun. 47 (2014) 17–20.
- [15] D. Arrigan, M. Ghita, V. Beni, Selective voltammetric detection of dopamine in the presence of ascorbate, Chem. Commun. 6 (2004) 732–733.
- [16] V. Beni, M. Ghita, D. Arrigan, Cyclic and pulse voltammetric study of dopamine at the interface between two immiscible electrolyte solutions, Biosens. Bioelectron. 20 (2005) 2097–2103.
- [17] D. Zhan, S. Mao, Q. Zhao, Z. Chen, H. Hu, P. Jing, M. Zhang, Z. Zhu, Y. Shao, Electro-chemical investigation of dopamine at the water/1,2-dichloroethane interface, Anal. Chem. 76 (2004) 4128–4136.
- [18] V. Marecek, Z. Samec, Electrolysis at the interface between two immiscible electrolyte solutions: determination of acetylcholine by differential pulse stripping voltammetry, Anal. Lett. 14 (1981) 1241–1253.
- [19] Y. Shao, H.H. Girault, Kinetics of the transfer of acetylcholine across the water + sucrose/1, 2-dichloroethane interface: a comparison between ion transport and ion transfer. J. Electroanal. Chem. 282 (1990) 59–72.
- [20] M.L. Colombo, S. McNeil, N. Iwai, A. Chang, M. Shen, Electrochemical detection of dopamine via assisted ion transfer at nanopipet electrode using cyclic voltammetry, J. Electrochem. Soc. 163 (2016) H3072–H3076.
- [21] M. Colombo, J. Sweedler, M. Shen, Nanopipet-based liquid–liquid interface probes for the electrochemical detection of acetylcholine, tryptamine, and serotonin via ionic transfer, Anal. Chem. 87 (2015) 5095–5100.
- [22] M. Shen, M. Colombo, Electrochemical nanoprobes for the chemical detection of neurotransmitters, Anal. Methods 7 (2015) 7095–7105.
- [23] T.J. Stockmann, A. Montgomery, Z.J. Ding, Determination of alkali metal ion transfers at liquid/liquid interfaces stabilized by a micropipette, Electroanal. Chem. 684 (2012) 6–12
- [24] D. Zhan, X. Li, W. Zhan, F. Fan, A.J. Bard, Scanning electrochemical microscopy. 58. Application of a micropipet-supported ITIES tip to detect Ag⁺ and study its effect on fibroblast cells, Anal, Chem. 79 (2007) 5225–5231.
- [25] U. Nestor, H. Wen, G. Girma, Z. Mei, W. Fei, Y. Yang, C. Zhang, D. Zhan, Facilitated Li⁺ ion transfer across the water/1,2-dichloroethane interface by the solvation effect, Chem. Commun. 50 (2014) 1015–1017.
- [26] Y. Shao, B. Liu, M.V. Mirkin, Studying ionic reactions by a new generation/collection technique, J. Am. Chem. Soc. 120 (1998) 12700–12701.
- [27] F.O. Laforge, P. Sun, M.V. Mirkin, Shuttling mechanism of ion transfer at the interface between two immiscible liquids, J. Am. Chem. Soc. 128 (2006) 15019–15025.
- [28] M. Shen, R. Ishimatsu, J. Kim, S. Amemiya, Quantitative imaging of ion transport through single nanopores by high-resolution scanning electrochemical microscopy, J. Am. Chem. Soc. 134 (2012) 9856–9859.
- [29] J. Kim, A. Izadyar, M. Shen, R. Ishimatsu, S. Amemiya, Ion permeability of the nuclear pore complex and ion-induced macromolecular permeation as studied by scanning electrochemical and fluorescence microscopy, Anal. Chem. 86 (2014) 2090–2098.
- [30] J. Kim, M. Shen, N. Nioradze, S. Amemiya, Stabilizing nanometer scale tip-to-substrate gaps in scanning electrochemical microscopy using an isothermal chamber for thermal drift suppression, Anal. Chem. 84 (2012) 3489–3492.
- [31] Y. Shao, M. Mirkin, Scanning electrochemical microscopy (SECM) of facilitated ion transfer at the liquid/liquid interface, J. Electroanal. Chem. 439 (1997) 137–143.
- [32] Y. Shao, M. Mirkin, Fast kinetic measurements with nanometer-sized pipets. transfer of potassium ion from water into dichloroethane facilitated by dibenzo-18-crown-6, J. Am. Chem. Soc. 119 (1997) 8103–8104.
- [33] F. Reymond, G. Lagger, P.-A. Carrupt, H. Girault, Facilitated ion transfer reactions across oil/water interfaces: Part II. Use of the convoluted current for the calculation of the association constants and for an amperometric determination of the stoichiometry of ML^z_j + complexes, J. Electroanal. Chem. 451 (1998) 59–76.
- [34] L. Tomaszewski, G. Lagger, H. Girault, Electrochemical extraction of Cu(I) and Cu(II) ions assisted by 1,4,7,10-tetrathiacyclododecane, Anal. Chem. 71 (1999) 837–841.
- [35] H. Bingol, E. Akgemci, M. Ersoz, T. Atalay, Electrochemical investigation of heavy metal ion transfer across the water/1,2-dichloroethane interface assisted by 9-ethyl-3carbazolecarboxaldehyde-thiosemicarbazone, Electroanalysis 19 (2007) 1327–1333.
- [36] R. Gulaboski, E. Ferreira, C. Pereira, M.N.D.S. Cordeiro, A. Garau, V. Lippolis, A.F. Silva, Coupling of cyclic voltammetry and electrochemical impedance spectroscopy for probing the thermodynamics of facilitated ion transfer reactions exhibiting chemical kinetic hindrances, J. Phys. Chem. C 112 (2008) 153–161.
- [37] G. Lagger, L. Tomaszewski, M.D. Osborne, B.J. Seddon, H.H. Girault, Electrochemical extraction of heavy metal ions assisted by cyclic thioether ligands, J. Electroanal. Chem. 451 (1998) 29–37.
- [38] Z. Samec, Electrochemistry at the interface between two immiscible electrolyte solutions (IUPAC Technical Report), Pure Appl. Chem. 76 (2004) 2147–2180.
- [39] Y. Shao, S.N. Tan, H.H. Girault, Ion transfer facilitated by the neutral carrier N, N,-Dicyclohexyl-N',N'-diisobutyl-cis-cyclohexane-1,2-dicarboxamide across the water/1,2dichloroethane interface, J. Chem. Soc. Faraday Trans. 89 (1993) 4307–4312.
- [40] Wandlowski T., Marecek V., Samec Z., Galvani potential scales for water-nitrobenzene and water-1,2-dichloroethane interfaces, Electrochim. Acta 35 (1990) 1173–1175.
- [41] D.R. Lide, CRC handbook of chemistry and physics (70th edition), CRC Press, Boca Raton, FL, 1990.
- [42] The Metabolomics Innovation Centre. http://www.hmdb.ca/metabolites/hmdb00112.
- [43] J. Sangster, Octanol-water partition coefficients of simple organic compounds, J. Phys. Chem. Ref. Data. 18 (1989) 1111.
- [44] D.C. Harris (Ed.), Quantitative Chemical Analysis, W. H. Freeman & Company, New York, NY 2016, pp. 163–166.
- [45] H.J. Buschmann, The macrocyclic and cryptate effect. 6 Complexation of protons by noncyclic polyethers and crown ethers in acetonitrile, Inorg. Chim. Acta 118 (1986) 77–80